
NEXT: Multi-Grained Mixture of Experts via Text-Modulation for Multi-Modal Object Re-ID

Shihao Li¹ Chenglong Li¹ Aihua Zheng^{1*} Andong Lu¹ Jin Tang¹ Jixin Ma²

¹Anhui University, China

²University of Greenwich, UK

¹{shli0603, lcl1314, ahzheng214, adlu_ah}@foxmail.com

¹tangjin@ahu.edu.cn, ²j.ma@greenwich.ac.uk

Abstract

Multi-modal object re-identification (ReID) aims to extract identity features across heterogeneous spectral modalities to enable accurate recognition and retrieval in complex real-world scenarios. However, most existing methods rely on implicit feature fusion structures, making it difficult to model fine-grained recognition strategies under varying challenging conditions. Benefiting from the powerful semantic understanding capabilities of Multi-modal Large Language Models (MLLMs), the visual appearance of an object can be effectively translated into descriptive text. In this paper, we propose a reliable multi-modal caption generation method based on attribute confidence, which significantly reduces the unknown recognition rate of MLLMs in multi-modal semantic generation and improves the quality of generated text. Additionally, we propose a novel ReID framework **NEXT**, the Multi-grained Mixture of Experts via Text-Modulation for Multi-modal Object Re-Identification. Specifically, we decouple the recognition problem into semantic and structural expert branches to separately capture modality-specific appearance and intrinsic structure. For semantic recognition, we propose the Text-Modulated Semantic-sampling Experts (TMSE), which leverages randomly sampled high-quality semantic texts to modulate expert-specific sampling of multi-modal features and mining intra-modality fine-grained semantic cues. Then, to recognize coarse-grained structure features, we propose the Context-Shared Structure-aware Experts (CSSE) that focuses on capturing the holistic object structure across modalities and maintains inter-modality structural consistency through a soft routing mechanism. Finally, we propose the Multi-Modal Feature Aggregation (MMFA), which adopts a unified feature fusion strategy to simply and effectively integrate semantic and structural expert outputs into the final identity representations. Extensive experiments on four common public datasets demonstrate the effectiveness of our method and show that it significantly outperforms existing state-of-the-art methods. [The source code will be released upon acceptance.](#)

1 Introduction

Object re-identification (ReID) aims to construct discriminative identity representations by capturing object characteristics such as appearance, clothing, body shape, and posture [1–7]. However, in real-world scenarios, variations in lighting, weather, occlusion, and clothing [8–11] hinder the performance of conventional ReID methods. To address these challenges, multi-modal object re-identification [12–15] has attracted increasing research interest in recent years. Benefit from the complementary advantages of different spectral modalities, identity information can be more

*Corresponding Author

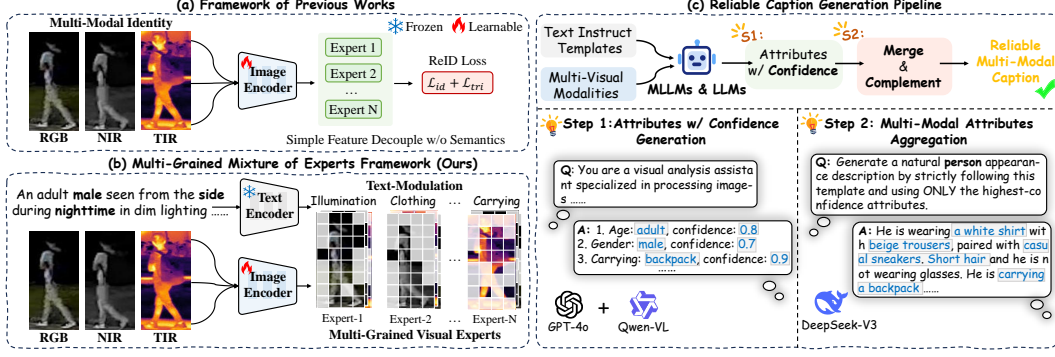


Figure 1: Motivation of our proposed method. Better view with color and zoom in.



Figure 2: Generated caption samples and text quality analysis on RGBNT201 dataset.

comprehensively captured. Despite this, intra-modal noise and inter-modal heterogeneity remain key obstacles to effective identity representation fusion. To overcome these issues, existing methods focus on implicit identity-level feature fusion [16–19], fine-grained feature complementarity [20, 21, 15], and frequency-domain interactions [22, 20]. However, semantic-aware fusion [23, 24] of multi-modal identity features is still underexplored.

Recent progress in vision-language models [25–29] has advanced visual understanding tasks, including object re-identification [30, 31]. Traditional ReID methods benefit from the latent alignment space between visual and linguistic modalities, enabling effective extraction of semantic identity representations [30, 31]. Recent research on learnable semantic prompts allows models to capture identity-relevant signals even in the absence of explicit semantic descriptions [32, 33, 24]. With the evolution of Multi-modal Large Language Models (MLLMs) [34–36], the ability to generate image-text pairs introduces new opportunities for object re-identification. Pioneering methods such as IDEA [23], TVI-LFM [37], and MP-ReID [38] integrate MLLMs into the ReID task by generating identity-relevant captions, thereby extending identity representations into the textual modality. For instance, IDEA [23] invests textual features into the visual representation space to capture cross-modal semantic information. However, the perception and fusion of fine-grained identity semantics across multi-modal data remain underexplored. Therefore, we raise the question: *Can we further modulate the model to perceive fine-grained multi-modal features under diverse identity semantics?*

Compared to labor-intensive human annotation, MLLMs can easily obtain textual descriptions of objects using instruction-based templates. However, in multi-modal scenarios, the appearance information of the object is often suppressed or distorted by various environmental conditions and noise. The IDEA [23] introduces a caption generation method combined with attribute-based refinement to leverage modal-specific descriptions. Nevertheless, it overlooks the accuracy of captions in low-quality modalities, leading to unreliable quantification of attributes. To tackle this, we propose

a reliable caption generation framework, as shown in Fig. 1(c). **Specifically, we decompose the caption generation into two steps: confidence-aware attribute generation and multi-modal attributes aggregation.** By enforcing the model to output a confidence score for each attribute, we encourage fine-grained evaluation and strengthen the expressiveness of each attribute. Based on the confidence scores, we quantify the attribute importance across different modalities, enabling us to complement missing semantic information through multi-modal captions. Finally, the aggregated attributes are passed to an LLM to flexibly generate the final textual captions.

High-quality captions effectively guide the model to focus on identity-relevant representations. **Building on this, we propose a multi-grained mixture of experts framework named NEXT, which models the identity recognition process through semantic-sampling and structure-aware experts.** The framework consists of three main components: Text-Modulated Semantic-sampling Experts (TMSE), Context-Shared Structure-aware Experts (CSSE), and Multi-Modal Feature Aggregation (MMFA). Specifically, TMSE samples fine-grained part-level features within each modality. The text modulation mechanism encourages the experts to focus on semantically relevant regions during training, thereby capturing intra-modality identity semantic features. Meanwhile, CSSE perceives inter-modality structural features of the object identity through a soft routing mechanism shared across modalities. Finally, MMFA unifies the features of different expert branches into a comprehensive multi-modal identity representation. Extensive experiments on four multi-modal object re-identification benchmarks demonstrate the effectiveness of our proposed approach.

The main contributions of this paper are summarized as follows:

- We propose a novel mixture of experts learning framework to learn comprehensive multi-modal identity representations for multi-modal object re-identification. It decomposes the identity modeling process into semantic and structural recognition to better leverage the complementary information across heterogeneous modalities.
- We propose the Text-Modulated Semantic-sampling Experts (TMSE) to model intra-modal feature sampling under diverse semantic challenges, the Context-Shared Structure-aware Experts (CSSE) to capture the complete inter-modal identity structure, and the Multi-Modal Feature Aggregation (MMFA) to integrate the outputs of multiple experts into a unified identity representation.
- We propose a novel and reliable multi-modal caption generation method that leverages attribute confidence to effectively harness MLLMs to expand four popular benchmarks with high-quality textual annotations. Extensive experiments are conducted on these benchmarks to validate the effectiveness of our method. The results demonstrated that the proposed method significantly outperformed the state-of-the-art methods.

2 Related Work

2.1 Multi-Modal Object Re-Identification

Multi-modal object ReID leverages the complementary imaging advantages of multi-spectra to enable robust identity recognition under adverse conditions. However, intra-modal noise and inter-modal spectral heterogeneity remain significant challenges. To fuse the heterogeneous visual features, TOP-ReID [16] proposes a modality permutation and reconstruction mechanism to align multi-modal representations. PromptMA [17] introduces a prompt-based token selection and fusion strategy to effectively integrate multi-modal features and suppress background interference. MambaPro [19] presents a selective state-space fusion approach based on Mamba [39] to aggregate intra- and inter-modal features. EDITOR [20] adopts frequency- and feature-based selection mechanisms to filter out background and low-quality noise. FACENet [15] utilizes illumination priors to enhance degraded modalities. TIENet [22] introduces an amplitude-guided phase learning strategy for frequency-domain enhancement. ICPL-ReID [24] applies an identity prototype-based conditional prompt learning method to guide semantic learning across modalities. IDEA [23] inverts textual features into the visual space to guide model learning, and captures discriminative local features across multi-modal via deformable aggregation. Despite these advancements, existing methods still lack a deep exploration of identity semantics and intrinsic structures. To bridge this gap, we propose a multi-grained mixture of experts via text-modulation that fuses features from different modalities through semantic and structural perspectives, aiming to enhance multi-modal identity representation.

2.2 Large Foundation Model in Re-Identification

The rise of MLLMs [35, 34, 36] significantly advances visual understanding tasks. Numerous studies demonstrate the effectiveness of MLLMs [40, 41] in generating high-quality text and robust generalization in vision-language alignment. Large-scale vision-language foundation models, such as CLIP [25], exhibit powerful visual perception and semantic understanding capabilities. Leveraging the latent image-text aligned space, researchers employ the learnable prompt [29, 28] to effectively adapt these models to classification, retrieval, and open-set recognition tasks. Methods like CLIP-ReID [30] and PromptSG [31] utilize learnable semantic prompts to transfer the CLIP [25] model to object re-identification tasks. Other approaches, such as MP-ReID [38], TVI-LFM [37], and IDEA [23], exploit MLLMs to generate identity-level textual descriptions from existing ReID datasets. However, these methods still lack reliable text generation under multi-modal conditions. Unlike IDEA [23], we further quantify attributes and propose a confidence-aware attribute generation strategy. We incorporate a multi-modal merging and complementation mechanism to achieve high-quality and reliable caption generation. Additionally, we introduce the NEXT framework, which leverages semantic experts to extract fine-grained multi-modal part features, aiming to tackle diverse semantic challenges in multi-modal scenarios.

2.3 Multi-Modal Mixture of Experts

Mixture-of-Experts (MoE) [42] achieves remarkable progress in both computer vision and natural language processing domains due to its flexible design and efficient activation mechanisms. In multi-modal visual tasks [43–46], MoE frameworks are typically designed with modality-shared and modality-specific experts to effectively capture diverse multi-modal features. However, these methods still fall short in learning identity-related representations for multi-modal object ReID. DeMo [18] first applies the MoE framework to the multi-modal ReID task by combining modality-specific experts to decouple shared and unique features. Despite this, it lacks fine-grained identity semantic understanding. To address this limitation, we propose text-modulated semantic-sampling experts and context-shared structure-aware experts to jointly capture semantic and structural features, enabling more comprehensive identity representation across multi-modalities.

3 Multi-Grained Mixture of Experts via Text-Modulation

In this section, we elaborate the proposed mixture-of-experts learning framework. As shown in Fig. 3 our proposed Multi-Grained Mixture-of-Experts framework includes the Text-Modulated Semantic-sampling Experts (TMSE) module, Context-Shared Structure-aware Experts (CSSE) module and Multi-Modal Feature Aggregation (MMFA) module.

Overview. We first define the basic notations and introduce the overall pipeline of the proposed framework. For multi-modal object ReID, each identity instance consists of three different modalities: visible light (RGB), near-infrared (NIR), and thermal infrared (TIR), denoted as $\mathbf{X}_I = [X_{I,rgb}, X_{I,nir}, X_{I,tir}]$. Benefiting from the strong visual understanding capabilities of Multi-modal Large Language Models (MLLMs), we input each modality image \mathbf{X}_I along with the modality-specific instruction template \mathbf{P}_M into the MLLM $\mathcal{M}(\cdot)$ to extract detailed identity appearance information $\mathbf{X}_T = [X_{T,rgb}, X_{T,nir}, X_{T,tir}]$. Supported by large-scale pretraining for vision-text alignment, CLIP effectively aligns image and text features within a shared latent space. We feed the visual modality \mathbf{X}_I into the CLIP visual encoder $\mathcal{V}(\cdot)$ to extract visual features $\mathbf{F}_{I,m} = [\mathbf{f}_{I,m}^{cls}; \mathbf{F}_{I,m}^{tok}] \in \mathbb{R}^{M \times (1+N) \times D}$, and input the object appearance description \mathbf{X}_T into the frozen CLIP text encoder $\mathcal{T}(\cdot)$ to extract textual features $\mathbf{F}_{T,m} = [\mathbf{f}_{T,m}^{cls}; \mathbf{F}_{T,m}^{tok}] \in \mathbb{R}^{M \times (1+L) \times D}$, where M is modality number, N is the length of visual patch tokens, L is the length of text patch tokens, D is the dimension length. As shown in Fig. 3(b), we define a set of semantic-sampling experts $\mathbf{E}_T = \{E_t^{(1)}, E_t^{(2)}, \dots, E_t^{(N_T)}\}$, where N_T denotes the number of semantic experts. Guided by high-quality textual features, each expert discards semantically irrelevant tokens and mines semantically related patch tokens within each modality. Meanwhile, as depicted in Fig. 3(d), we introduce another set of structure-aware experts $\mathbf{E}_C = \{E_c^{(1)}, E_c^{(2)}, \dots, E_c^{(N_C)}\}$, where N_C denotes the number of structure experts. These experts jointly utilize all patch features and adopt a soft routing mechanism to perceive the structural consistency of objects across modalities. Finally, we aggregate the features captured by all experts, including \mathbf{E}_T and \mathbf{E}_C , through the multi-modal feature aggregation module to form a unified multi-modal representation as the final discriminative feature.

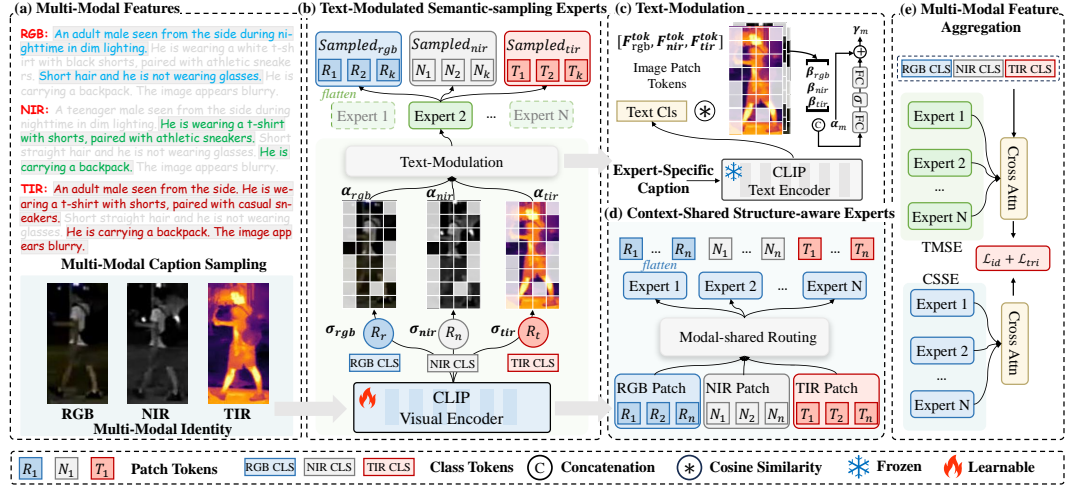


Figure 3: Framework of our proposed method.

3.1 Text-Modulated Semantic-sampling Experts (TMSE)

In practical scenarios, challenges such as illumination variations, background interference, and low-quality noise often affect different local regions across modalities. This necessitates overcoming modality heterogeneity and discovering complementary cross-modal features. However, existing approaches often lack explicit semantic guidance. To address this, we leverage the object-level textual semantics \mathbf{X}_T extracted from MLLMs to guide a set of semantic experts $\mathbf{E}_T = \{E_t^{(1)}, E_t^{(2)}, \dots, E_t^{(N_T)}\}$ in dynamically sampling semantic-related local features across different modalities, to tackle various semantic challenges. The structure of each expert is defined as:

$$E_t(\mathbf{F}) = \text{Dropout}(\text{MLP}(\text{LN}(\mathbf{F}))) + \mathbf{F}, \quad (1)$$

where \mathbf{F} denotes the input features, LN is a layer normalization, MLP is a multilayer perceptron, and Dropout is applied to prevent overfitting.

Dynamic Sampling Route. To sample semantic features from each modality, we design a set of modality-specific sampling routes for each expert, denoted as $\mathbf{R}_m = [\mathbf{R}_{rgb}, \mathbf{R}_{nir}, \mathbf{R}_{tir}]$. As shown in Eq.(2), we encode the patch-level features $\mathbf{F}_{I,m}^{\text{tok}}$ into the routing matrix α_m , and map the class token $\mathbf{f}_{I,m}^{\text{cls}}$ into the scalar threshold σ_m . The formulation is as follows:

$$\alpha_m = \text{FC}(\delta(\text{FC}(\mathbf{F}_{I,m}^{\text{tok}}))), \quad \sigma_m = \text{FC}(\delta(\text{FC}(\mathbf{f}_{I,m}^{\text{cls}}))), \quad \alpha_m \in \mathbb{R}^{H \times W}, \sigma_m \in \mathbb{R}. \quad (2)$$

$$\mathbf{M}_m(i, j) = \begin{cases} 1, & \text{if } \alpha_m(i, j) > \sigma_m, \\ 0, & \text{otherwise} \end{cases}, \quad \text{for } i = 1, \dots, H, j = 1, \dots, W \quad (3)$$

As shown in Eq.(3), we assign 1 to entries in α_m that exceed the threshold σ_m and 0 otherwise, to discard irrelevant features while keeping the operation differentiable.

Multi-Grained Text Modulation. To empower the semantic awareness of each expert, we employ random semantic text prompts during training, guiding each expert toward distinct semantic challenges. Formally, the raw semantic description is decomposed into fine-grained sentences for each modality: $X_{T,m} = \{s_m^{(1)}, s_m^{(2)}, \dots, s_m^{(n_m)}\}$, $m \in \{\text{rgb}, \text{nir}, \text{tir}\}$, where n_m is the maximum number of sentences. For each expert $E_t^{(i)}$, we randomly select a subset $\hat{X}_{T,m}^{(i)}$ from $X_{T,m}$ as its semantic modulation signal. The sampling process is defined as:

$$\hat{\mathbf{X}}_T^{(i)} = [\hat{X}_{T,rgb}^{(i)}, \hat{X}_{T,nir}^{(i)}, \hat{X}_{T,tir}^{(i)}], \quad \hat{X}_{T,m}^{(i)} \sim \text{Sampling}(X_{T,m}) \quad (4)$$

where i denotes the i -th semantic experts, and **Sampling** is a random probability distribution.

To modulate the visual sampling route, we first encode the randomly sampled high-quality semantic text into the visual-text latent space as text feature vector $\mathbf{f}_{T,m}^{\text{cls}}$. Then, we compute the cosine similarity between this text vector and the visual patch tokens to obtain the semantic relevance matrix β_m :

$$\beta_m = \frac{\mathbf{f}_{\hat{T},m}^{\text{cls}} \cdot \mathbf{F}_{I,m}^{\text{tok}}}{\|\mathbf{f}_{\hat{T},m}^{\text{cls}}\|_2 \cdot \|\mathbf{F}_{I,m}^{\text{tok}}\|_2}, \quad \beta_m \in \mathbb{R}^{H \times W}. \quad (5)$$

We then integrate this semantic guidance with the route matrix α_m to produce the modulation matrix γ_m , as formulated below:

$$\gamma_m = \text{Modulation}(\alpha_m, \beta_m) + \alpha_m, \quad \gamma_m \in \mathbb{R}^{H \times W} \quad (6)$$

where **Modulation** refers to the modulation network whose structure is illustrated in Fig. 3(c).

Finally, we replace the route matrix α_m in Eq.(3) with the modulated matrix γ_m to obtain the final modulation-based sampling matrix $\hat{\mathbf{M}}_m$.

$$\hat{\mathbf{F}}_I = \text{Concat}(\hat{\mathbf{M}}_m \odot \hat{\mathbf{F}}_{I,m}^{\text{tok}}), \quad \hat{\mathbf{F}}_{I,m}^{\text{tok}} = E_t(\mathbf{F}_{I,m}^{\text{tok}}), \quad \forall m \in \{\text{rgb}, \text{nir}, \text{tir}\} \quad (7)$$

As shown in the Eq.(7) above, $\hat{\mathbf{M}}_m$ dynamically samples the informative features for each semantic expert $E_t^{(i)}$ within a modality. These sampled features are concatenated to obtain the final multi-modal semantic feature $\hat{\mathbf{F}}_I$.

3.2 Context-Shared Structure-aware Experts (CSSE)

Although semantic experts focus on fine-grained part sampling under various semantic challenges. The identity recognition and discrimination still rely on the structural integrity of the object. To this end, we introduce a set of structure experts, denoted as $\mathbf{E}_C = \{E_c^{(1)}, E_c^{(2)}, \dots, E_c^{(N_C)}\}$, to comprehensively perceive the holistic object structure across modalities.

Specifically, to preserve structural integrity, we first concatenate multi-modal patch features as $\mathbf{F}_I^{\text{tok}} = \text{Concat}(\mathbf{F}_{I,\text{rgb}}^{\text{tok}}, \mathbf{F}_{I,\text{nir}}^{\text{tok}}, \mathbf{F}_{I,\text{tir}}^{\text{tok}})$, and then feed them into a modality-shared routing network R_s to compute the expert fusion weights as follows:

$$\omega = \text{Softmax}(\text{FC}(\mathbf{F}_I^{\text{tok}})), \quad \omega \in \mathbb{R}^{N_C} \quad (8)$$

where **FC** denotes the fully connected layer, and **Softmax** encodes the expert selection weights, resulting in the soft routing matrix ω .

Finally, we feed the concatenated multi-modal token features into the structure experts module \mathbf{E}_C and compute the final multi-modal structural representation by weighting each output of expert using the soft routing matrix ω . The process is formulated as follows:

$$\tilde{\mathbf{F}}_I = \sum_{i=1}^{N_C} \omega_i \cdot E_c^{(i)}(\mathbf{F}_I^{\text{tok}}), \quad \tilde{\mathbf{F}}_I^{\text{tok}} = \{E_c^{(i)}(\mathbf{F}_I^{\text{tok}}) \mid i = 1, 2, \dots, N_C\}, \quad (9)$$

where $\tilde{\mathbf{F}}_I$ is represent the final multi-modal structure feature.

3.3 Multi-Modal Feature Aggregation (MMFA)

Experts of different types mine various identity features. The semantic expert \mathbf{E}_T extracts fine-grained semantic features $\hat{\mathbf{F}}_I^{(i)}$, and the structural expert \mathbf{E}_C captures structural consistency features $\tilde{\mathbf{F}}_I$. As illustrated in Fig. 3(e), we combine these features to form the complete object identity feature set $\mathbf{F}_I^{\text{exp}} = [\hat{\mathbf{F}}_I^{(1)}, \hat{\mathbf{F}}_I^{(2)}, \dots, \hat{\mathbf{F}}_I^{(N_T)}; \tilde{\mathbf{F}}_I]$. The modality class tokens are concatenated to form the modality query features $\mathbf{f}_I^{\text{cls}} = \text{Concat}(\mathbf{f}_{I,\text{rgb}}^{\text{cls}}, \mathbf{f}_{I,\text{nir}}^{\text{cls}}, \mathbf{f}_{I,\text{tir}}^{\text{cls}})$. Following this, we treat $\mathbf{f}_I^{\text{cls}}$ as the query feature Q and the expert features as the key K and value V . Through the Cross-Attention mechanism, we obtain the multi-modal representation for each expert and concatenate them to form the final identity representation $\hat{\mathbf{f}}_I^{\text{cls}}$. The process is formulated as follows:

$$\hat{\mathbf{f}}_I^{\text{cls}} = \text{Concat}(\hat{\mathbf{f}}_I^{\text{cls}(1)}, \hat{\mathbf{f}}_I^{\text{cls}(2)}, \dots, \hat{\mathbf{f}}_I^{\text{cls}(N_T)}, \tilde{\mathbf{f}}_I^{\text{cls}}), \quad (10)$$

$$\hat{\mathbf{f}}_I^{\text{cls}(i)} = \text{FFN}(\text{LN}(\text{CA}(\mathbf{f}_I^{\text{cls}}, \mathbf{F}_I^{\text{exp}(i)}))), \quad \text{for } i = 1, \dots, N_T + 1. \quad (11)$$

where **CA** is the Cross-Attention mechanism, and **FFN** is the feedback forward layer.

Table 1: Comparison with the state-of-the-art methods on RGBNT201. The best and second best results are marked in **bold** and underline, respectively.

| Methods | Venue | Structure | RGBNT201 | | | |
|----------------|-------------|-----------|-------------|-------------|-------------|-------------|
| | | | mAP | R-1 | R-5 | R-10 |
| HAMNet [12] | AAAI20 | CNN | 27.7 | 26.3 | 41.5 | 51.7 |
| PFNet [14] | AAAI21 | CNN | 38.5 | 38.9 | 52.0 | 58.4 |
| IEEE [47] | AAAI22 | CNN | 46.4 | 47.1 | 58.5 | 64.2 |
| TIENet [22] | TNNLS25 | CNN | 54.4 | 54.4 | 66.3 | 71.1 |
| UniCat [48] | NIPSW23 | CNN | 57.0 | 55.7 | - | - |
| HTT [49] | AAAI24 | ViT | 71.1 | 73.4 | 83.1 | 87.3 |
| TOP-ReID [16] | AAAI24 | ViT | 72.3 | 76.6 | 84.7 | 89.4 |
| EDITOR [20] | CVPR24 | ViT | 66.5 | 68.3 | 81.1 | 88.2 |
| WTSF-ReID [50] | ESWA25 | ViT | 67.9 | 72.2 | 83.4 | 89.7 |
| ICPL-ReID [24] | TMM25 | CLIP | 75.1 | 77.4 | 84.2 | 87.9 |
| PromptMA [17] | TIP25 | CLIP | 78.4 | 80.9 | 87.0 | 88.9 |
| MambaPro [19] | AAAI25 | CLIP | 78.9 | <u>83.4</u> | 89.8 | 91.9 |
| DeMo [18] | AAAI25 | CLIP | 79.0 | <u>82.3</u> | 88.8 | 92.0 |
| IDEA [23] | CVPR25 | CLIP | <u>80.2</u> | 82.1 | <u>90.0</u> | <u>93.3</u> |
| NEXT | Ours | CLIP | 82.4 | 86.6 | 92.0 | 94.7 |

3.4 Optimization and Inference

In line with prior work [3, 5], we use the object identity ID label as the ground-truth to train the classification loss L_{id} , and adopt the triplet loss L_{tri} to enhance identity compactness and separability. The final loss function is defined as:

$$L_{\text{final}}(\hat{\mathbf{f}}_I^{\text{cls}}) = L_{\text{id}}(\hat{\mathbf{f}}_I^{\text{cls}}) + L_{\text{tri}}(\hat{\mathbf{f}}_I^{\text{cls}}). \quad (12)$$

4 Experiment

4.1 Datasets and Evaluation Protocols

Datasets. We evaluate our method on four multi-modal object ReID datasets: RGBNT201 [14], MSVR310 [13], RGBNT100 [12], and WMVEID863 [15]. To extend these datasets, we employ GPT-4o [34] and Qwen-VL [35] to automatically generate object attribute with confidence, and DeepSeek-V3 [51] to compose the final caption for each image modality in the train and test sets. Details of dataset scales and implementation details are provided in the Appendix A.

Evaluation Protocols. In line with the convention of the ReID community [3, 1], we use Rank-K ($K = 1, 5, 10$) matching accuracy and the Mean Average Precision (mAP) as evaluation metrics. As in previous works [14, 12, 15], we adopt the common evaluation protocol for RGBNT201 [14], RGBNT100 [12] and WMVEID863 [15]. For MSVR310 [13], we enforce a strict protocol [13] that filters out samples with the same identity and time span based on time labels to avoid easy matching.

4.2 Comparison with State-of-the-Art Methods

Performance on Person Dataset. In Table 1, we compare our NEXT with existing multi-modal methods on RGBNT201 [14] dataset. Benefiting from the flexible fusion of semantic and structure experts, our method achieves a significant performance lead, reaching **82.4%/86.6%** mAP/Rank-1 accuracy. Compared with DeMo [18], which adopts MoE structure to handle modality-shared and modality-specific features, our method demonstrates superior performance by perceiving both the semantic and structural features of the objects. Against IDEA [23], which utilizes semantic inversion and deformable offset sampling, our method leverages text-modulation to guide expert sampling multi-modal semantic, improving mAP and Rank-1 by **+2.2%** and **+4.5%**, respectively. These results validate the effectiveness of NEXT in learning more discriminative multi-modal identity features through textual semantics.

Table 2: Comparison with the state-of-the-art methods on MSVR310, RGBNT100 and WMVEID863.

| Methods | Venue | Strucutre | MSVR310 | | RGBNT100 | | WMVEID863 | | | |
|----------------|-------------|-------------|-------------|-------------|-------------|-------------|-------------|-------------|-------------|-------------|
| | | | mAP | R-1 | mAP | R-1 | mAP | R-1 | R-5 | R-10 |
| HAMNet [12] | AAAI20 | CNN | 27.1 | 42.3 | 74.5 | 93.3 | 45.6 | 48.5 | 63.1 | 68.8 |
| PFNet [14] | AAAI21 | CNN | 23.5 | 37.4 | 68.1 | 94.1 | 50.1 | 55.9 | 68.7 | 75.1 |
| IEEE [47] | AAAI22 | CNN | 21.0 | 41.0 | 61.3 | 87.8 | 45.9 | 48.6 | 64.3 | 67.9 |
| CCNet [13] | INFFUS23 | CNN | 36.4 | 55.2 | 77.2 | 96.3 | 50.3 | 52.7 | 69.6 | 75.1 |
| TOP-ReID [16] | AAAI24 | ViT | 35.9 | 44.6 | 81.2 | 96.4 | 67.7 | 75.3 | 80.8 | 83.5 |
| FACENet [15] | INFFUS25 | ViT | 36.2 | 54.1 | 81.5 | 96.9 | 69.8 | 77.0 | 81.0 | 84.2 |
| EDITOR [20] | CVPR24 | ViT | 39.0 | 49.3 | 82.1 | 96.4 | 65.6 | 73.8 | 80.0 | 82.3 |
| MambaPro [19] | AAAI25 | CLIP | 47.0 | 56.5 | 83.9 | 94.7 | 69.5 | 76.9 | 80.6 | 83.8 |
| PromptMA [17] | TIP25 | CLIP | 55.2 | 64.5 | 85.3 | 97.4 | - | - | - | - |
| DeMo [18] | AAAI25 | CLIP | 49.2 | 59.8 | 86.2 | 97.6 | 68.8 | 77.2 | 81.5 | 83.8 |
| IDEA [23] | CVPR25 | CLIP | 47.0 | 62.4 | 87.2 | 96.5 | - | - | - | - |
| ICPL-ReID [24] | TMM25 | CLIP | 56.9 | 77.7 | 87.0 | 98.6 | 67.2 | 74.0 | 81.3 | 85.6 |
| NEXT | Ours | CLIP | 60.8 | 79.0 | 88.2 | 97.7 | 70.9 | 77.8 | 84.3 | 86.7 |

Table 3: Ablation studies of different modules.

| | Modules | | | Metrics | |
|---|---------|------|------|-------------|-------------|
| | MMFA | TMSE | CSSE | mAP | R-1 |
| A | ✗ | ✗ | ✗ | 71.0 | 73.6 |
| B | ✓ | ✗ | ✗ | 74.2 | 76.6 |
| C | ✓ | ✓ | ✗ | 78.9 | 84.4 |
| D | ✓ | ✓ | ✓ | 82.4 | 86.6 |

Table 4: Effectiveness of different route strategy.

| | | Router Type | | Metrics | |
|---|---|-------------|-------|-------------|-------------|
| | | E_T | E_C | mAP | R-1 |
| A | ✗ | ✗ | ✗ | 78.3 | 82.5 |
| B | ✓ | ✗ | ✗ | 78.7 | 83.4 |
| C | ✓ | ✓ | ✓ | 80.3 | 84.3 |
| D | ✗ | ✓ | ✓ | 82.4 | 86.6 |

Table 5: Effectiveness of caption quality.

| Methods | Quality | mAP | R-1 |
|---------|---------|-------------|-------------|
| IDEA | 35% | 76.1 | 77.9 |
| | 70% | 78.1 | 79.9 |
| | 100% | 80.2 | 84.0 |
| Ours | 35% | 77.1 | 79.7 |
| | 70% | 80.0 | 82.2 |
| | 100% | 82.4 | 86.6 |

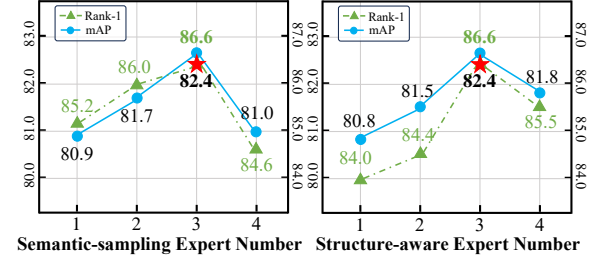


Figure 4: Effectiveness of the number of experts.

Performance on Vehicle Dataset. Table 2 outlines the performance of our method on vehicle ReID datasets. On the MSVR310 [13] dataset, our approach significantly outperforms existing methods, achieving **60.8% / 79.0%** mAP/Rank-1 accuracy, attributed to its semantic sampling and structural perception. On the RGBNT100 [12] dataset, our method continues to lead in mAP performance. For the challenging WMVEID863 dataset, where lighting variations degrade recognition performance, our method still improves over FACENet by **+1.1% / +0.8%** mAP/Rank-1. These results confirm the strong generalization and robustness of NEXT in vehicle ReID under complex conditions.

4.3 Ablation Studies

On the RGBNT201 [14] dataset, we thoroughly evaluation the effectiveness of each proposed module. Starting from a baseline built on a three-branch CLIP [25] visual backbone, we incrementally incorporate our components and remove them individually to investigate their specific contributions to the model’s overall performance. More experiments are available in the Appendix B.

Effectiveness of Key Modules. As shown in Table 7, the baseline (Row A) achieves **71.0%** mAP and **73.6%** Rank-1. In Row B, the MMFA improves performance by **+3.2% / +3.0%** by fusing baseline features as a single expert. Adding the TMSE module in Row C boosts accuracy to **78.9%** mAP and **84.4%** Rank-1 under semantic modulation. With the CSSE in Row D, the model gains performance **+2.5% / +2.2%** in mAP/Rank-1. These results confirm the contribution of each module to the overall performance.

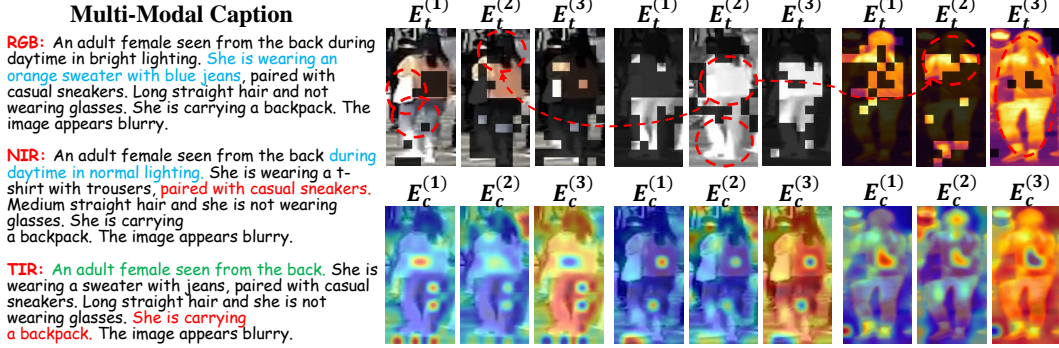


Figure 5: Visualization of the sampled patch tokens and activated feature regions for experts.

Effectiveness of Route Strategy. As shown in Table 4, using modality-specific routing for both experts (Row A) results in **78.3%/82.5%** mAP/Rank-1. Sharing routing for the semantic experts (Row B) slightly improves performance to **78.7%/83.4%**. When the structural experts adopt modality-shared routing (Row C), the model gains an additional **+1.6%/+0.9%**. In Row D, reverting the semantic expert to modality-specific routing further improves the results, showing that intra-modal semantic focus helps tackle semantic challenges more effectively.

Effectiveness of Caption Quality. In Table 5, we evaluate how text quality affects model performance by corrupting the captions with varying levels of noise. At 100% text quality, all models reach optimal accuracy, with IDEA achieving its best Rank-1 score. However, as quality degrades to 70%, performance drops significantly. When only 35% of the original text remains, IDEA falls to **76.1%/77.9%** (mAP/Rank-1), and NEXT to **77.1%/79.7%**. This highlights the strong dependency of semantic-guided methods on high-quality text.

Effectiveness of Experts Number. Fig. 4 illustrates how varying the number of experts influences model accuracy. With few experts, the model struggles to learn rich semantic information or recognize structural identity cues, which hampers overall performance. Conversely, an excessive number of experts causes redundancy and ambiguity in semantic-structural fusion, impairing identity representation. The results suggest that an appropriately chosen number of experts offers the best trade-off and leads to optimal performance.

4.4 Visualization Analysis

Expert Feature Visualization. As shown in Fig. 5, we visualize the sampling masks of the semantic experts and the activation maps of the structural experts. We observe that different semantic experts $E_t^{(i)}$ exhibit distinct modality preferences: for instance, $E_t^{(1)}$ tends to sample features from the RGB modality, $E_t^{(2)}$ from the NIR modality, and $E_t^{(3)}$ from the TIR modality. These sampling patterns are notably complementary across modalities, indicating that the semantically modulated expert network effectively learns complementary modality-specific features to enhance unimodal representations. Structural experts, on the other hand, maintain the integrity of coarse-grained identity structures. The parts ignored by expert $E_c^{(3)}$ are well captured by other structural experts. These observations validate that NEXT successfully decouples identity recognition into semantic sampling and structure modeling. More visualization results are provided in the Appendix D.

5 Conclusion

In this paper, we focus on the semantic learning of multi-modal object ReID. We first propose a reliable multi-modal caption generation approach based on MLLMs, which use confidence-aware attribute prompts to construct structured attribute sets, and quantitatively merge multi-modal attributes to compose high-quality captions. Additionally, we propose the NEXT, a novel multi-grained MoE network for multi-modal ReID. We decouple the recognition problem into fine-grained semantic sampling and coarse-grained structural perception to overcome modality heterogeneity and achieve discriminative identity representations. Specifically, we propose Text-Modulated Semantic-sampling Experts (TMSE) to perceive fine-grained identity semantics and dynamically sample semantic parts. Then, we propose Context-Shared Structure-aware Experts (CSSE) to capture coarse-grained structural cues via modality-shared routing. Finally, we incorporate a Multi-Modal Feature Aggregation (MMFA) module to unify features from various experts and obtain complete identity representations. Extensive experiments on four popular benchmarks demonstrate the effectiveness of our method.

References

- [1] Q. Leng, M. Ye, and Q. Tian, “A survey of open-world person re-identification,” *IEEE Transactions on Circuits and Systems for Video Technology*, vol. 30, no. 4, pp. 1092–1108, 2020.
- [2] M. Ye, J. Shen, G. Lin, T. Xiang, L. Shao, and S. C. H. Hoi, “Deep learning for person re-identification: A survey and outlook,” *IEEE Transactions on Pattern Analysis and Machine Intelligence*, vol. 44, no. 6, pp. 2872–2893, 2022.
- [3] S. He, H. Luo, P. Wang, F. Wang, H. Li, and W. Jiang, “Transreid: Transformer-based object re-identification,” in *Proceedings of the IEEE/CVF International Conference on Computer Vision*, 2021, pp. 14 993–15 002.
- [4] L. Zheng, L. Shen, L. Tian, S. Wang, J. Wang, and Q. Tian, “Scalable person re-identification: A benchmark,” in *Proceedings of the IEEE/CVF International Conference on Computer Vision*, 2015, pp. 1116–1124.
- [5] H. Luo, Y. Gu, X. Liao, S. Lai, and W. Jiang, “Bag of tricks and a strong baseline for deep person re-identification,” in *Proceedings of the IEEE/CVF Conference on Computer Vision and Pattern Recognition Workshops*, 2019, pp. 1487–1495.
- [6] K. Zhou, Y. Yang, A. Cavallaro, and T. Xiang, “Omni-scale feature learning for person re-identification,” in *Proceedings of the IEEE/CVF International Conference on Computer Vision*, 2019, pp. 3702–3712.
- [7] H. Li, A. Zheng, L. Sun, and Y. Luo, “Camera topology graph guided vehicle re-identification,” *IEEE Transactions on Multimedia*, vol. 26, pp. 1565–1577, 2024.
- [8] G. Wang, Y. Yuan, X. Chen, J. Li, and X. Zhou, “Learning discriminative features with multiple granularities for person re-identification,” in *Proceedings of the ACM International Conference on Multimedia*, 2018, pp. 274–282.
- [9] Y. Sun, L. Zheng, Y. Yang, Q. Tian, and S. Wang, “Beyond part models: Person retrieval with refined part pooling (and A strong convolutional baseline),” in *Proceedings of the European Conference on Computer Vision*, 2018, pp. 480–496.
- [10] A. Lu, Z. Zhang, Y. Huang, Y. Zhang, C. Li, J. Tang, and L. Wang, “Illumination distillation framework for nighttime person re-identification and a new benchmark,” *IEEE Transactions on Multimedia*, pp. 1–14, 2023.
- [11] W. Chen, I. Chen, C. Yeh, H. Yang, J. Ding, and S. Kuo, “Sjdl-vehicle: Semi-supervised joint defogging learning for foggy vehicle re-identification,” in *Proceedings of the AAAI Conference on Artificial Intelligence*, vol. 36, no. 1, 2022, pp. 347–355.
- [12] H. Li, C. Li, X. Zhu, A. Zheng, and B. Luo, “Multi-spectral vehicle re-identification: A challenge,” in *Proceedings of the AAAI Conference on Artificial Intelligence*, 2020, pp. 11 345–11 353.
- [13] A. Zheng, X. Zhu, Z. Ma, C. Li, J. Tang, and J. Ma, “Cross-directional consistency network with adaptive layer normalization for multi-spectral vehicle re-identification and a high-quality benchmark,” *Information Fusion*, vol. 100, p. 101901, 2023.
- [14] A. Zheng, Z. Wang, Z. Chen, C. Li, and J. Tang, “Robust multi-modality person re-identification,” in *Proceedings of the AAAI Conference on Artificial Intelligence*, 2021, pp. 3529–3537.
- [15] A. Zheng, Z. Ma, Y. Sun, Z. Wang, C. Li, and J. Tang, “Flare-aware cross-modal enhancement network for multi-spectral vehicle re-identification,” *Information Fusion*, vol. 116, p. 102800, 2025.
- [16] Y. Wang, X. Liu, P. Zhang, H. Lu, Z. Tu, and H. Lu, “Top-reid: Multi-spectral object re-identification with token permutation,” in *Proceedings of the AAAI Conference on Artificial Intelligence*, 2024, pp. 5758–5766.
- [17] S. Zhang, W. Luo, D. Cheng, Y. Xing, G. Liang, P. Wang, and Y. Zhang, “Prompt-based modality alignment for effective multi-modal object re-identification,” *IEEE Transactions on Image Processing*, pp. 1–1, 2025.
- [18] Y. Wang, Y. Liu, A. Zheng, and P. Zhang, “Demo: Decoupled feature-based mixture of experts for multi-modal object re-identification,” in *Proceedings of the AAAI Conference on Artificial Intelligence*, 2025.
- [19] Y. Wang, X. Liu, T. Yan, Y. Liu, A. Zheng, P. Zhang, and H. Lu, “Mambapro: Multi-modal object re-identification with mamba aggregation and synergistic prompt,” in *Proceedings of the AAAI Conference on Artificial Intelligence*, 2025.

[20] P. Zhang, Y. Wang, Y. Liu, Z. Tu, and H. Lu, “Magic tokens: Select diverse tokens for multi-modal object re-identification,” in *Proceedings of the IEEE/CVF Conference on Computer Vision and Pattern Recognition*, 2024, pp. 17 117–17 126.

[21] Z. Yu, Z. Huang, M. Hou, J. Pei, Y. Yan, Y. Liu, and D. Sun, “Representation selective coupling via token sparsification for multi-spectral object re-identification,” *IEEE Transactions on Circuits and Systems for Video Technology*, 2024.

[22] X. Yang, W. Dong, D. Cheng, N. Wang, and X. Gao, “Tinet: A tri-interaction enhancement network for multimodal person reidentification,” *IEEE Transactions on Neural Networks and Learning Systems*, 2025.

[23] Y. Wang, Y. Lv, P. Zhang, and H. Lu, “Idea: Inverted text with cooperative deformable aggregation for multi-modal object re-identification,” 2025.

[24] S. Li, A. Zheng, C. Li, J. Tang, and B. Luo, “Icpl-reid: Identity-conditional prompt learning for multi-spectral object re-identification,” *IEEE Transactions on Multimedia*, 2025.

[25] A. Radford, J. W. Kim, C. Hallacy, A. Ramesh, G. Goh, S. Agarwal, G. Sastry, A. Askell, P. Mishkin, J. Clark, G. Krueger, and I. Sutskever, “Learning transferable visual models from natural language supervision,” in *Proceedings of the International conference on machine learning*, vol. 139, 2021, pp. 8748–8763.

[26] J. Li, D. Li, C. Xiong, and S. C. H. Hoi, “BLIP: bootstrapping language-image pre-training for unified vision-language understanding and generation,” in *Proceedings of the International conference on machine learning*, vol. 162, 2022, pp. 12 888–12 900.

[27] L. H. Li, P. Zhang, H. Zhang, J. Yang, C. Li, Y. Zhong, L. Wang, L. Yuan, L. Zhang, J. Hwang, K. Chang, and J. Gao, “Grounded language-image pre-training,” in *Proceedings of the IEEE/CVF Conference on Computer Vision and Pattern Recognition*, 2022, pp. 10 955–10 965.

[28] K. Zhou, J. Yang, C. C. Loy, and Z. Liu, “Conditional prompt learning for vision-language models,” in *Proceedings of the IEEE/CVF Conference on Computer Vision and Pattern Recognition*, 2022, pp. 16 816–16 825.

[29] K. Zhou, J. Yang, C. C. Loy, and Z. Liu, “Learning to prompt for vision-language models,” *International Journal of Computer Vision*, vol. 130, no. 9, pp. 2337–2348, 2022.

[30] S. Li, L. Sun, and Q. Li, “Clip-reid: Exploiting vision-language model for image re-identification without concrete text labels,” in *Proceedings of the AAAI Conference on Artificial Intelligence*, 2023, pp. 1405–1413.

[31] Z. Yang, D. Wu, C. Wu, Z. Lin, J. Gu, and W. Wang, “A pedestrian is worth one prompt: Towards language guidance person re- identification,” in *Proceedings of the IEEE/CVF Conference on Computer Vision and Pattern Recognition*, 2024, pp. 17 343–17 353.

[32] J. Xu, Q. Wang, X. Xiong, D. Gai, R. Zhou, and D. Wang, “Clip-driven view-aware prompt learning for unsupervised vehicle re-identification,” in *Proceedings of the AAAI Conference on Artificial Intelligence*, 2025, pp. 8896–8904.

[33] W. Dai, L. Lu, and Z. Li, “Diffusion-based synthetic data generation for visible-infrared person re-identification,” in *Proceedings of the AAAI Conference on Artificial Intelligence*, 2025, pp. 11 185–11 193.

[34] A. Hurst, A. Lerer, A. P. Goucher, A. Perelman, A. Ramesh, A. Clark, A. Ostrow, A. Welihinda, A. Hayes, A. Radford, *et al.*, “Gpt-4o system card,” *arXiv preprint arXiv:2410.21276*, 2024.

[35] J. Bai, S. Bai, S. Yang, S. Wang, S. Tan, P. Wang, J. Lin, C. Zhou, and J. Zhou, “Qwen-vl: A versatile vision-language model for understanding, localization, text reading, and beyond,” 2023.

[36] H. Liu, C. Li, Q. Wu, and Y. J. Lee, “Visual instruction tuning,” in *NeurIPS*, 2023.

[37] Z. Hu, B. Yang, and M. Ye, “Empowering visible-infrared person re-identification with large foundation models,” in *Advances in Neural Information Processing Systems*, 2024.

[38] Y. Zhai, Y. Zeng, Z. Huang, Z. Qin, X. Jin, and D. Cao, “Multi-prompts learning with cross-modal alignment for attribute-based person re-identification,” in *Proceedings of the AAAI Conference on Artificial Intelligence*, 2024, pp. 6979–6987.

[39] A. Gu and T. Dao, “Mamba: Linear-time sequence modeling with selective state spaces,” *arXiv preprint arXiv:2312.00752*, 2023.

[40] W. Dai, J. Li, D. Li, A. M. H. Tiong, J. Zhao, W. Wang, B. Li, P. Fung, and S. C. H. Hoi, “Instructblip: Towards general-purpose vision-language models with instruction tuning,” in *NeurIPS*, 2023.

[41] Y. Liu, P. Chen, J. Cai, X. Jiang, Y. Hu, J. Yao, Y. Wang, and W. Xie, “Lamra: Large multimodal model as your advanced retrieval assistant,” vol. abs/2412.01720, 2024.

[42] R. A. Jacobs, M. I. Jordan, S. J. Nowlan, and G. E. Hinton, “Adaptive mixtures of local experts,” *Neural Comput.*, vol. 3, no. 1, pp. 79–87, 1991.

[43] C. Wu, Z. Shuai, Z. Tang, L. Wang, and L. Shen, “Dynamic modeling of patients, modalities and tasks via multi-modal multi-task mixture of experts,” in *Proceedings of the International Conference on Learning Representations*, 2025.

[44] H. Zhong, J. Chen, Y. Zhang, D. Huang, and Y. Wang, “Transforming vision transformer: Towards efficient multi-task asynchronous learner,” in *NeurIPS*, 2024.

[45] S. Yun, I. Choi, J. Peng, Y. Wu, J. Bao, Q. Zhang, J. Xin, Q. Long, and T. Chen, “Flex-moe: Modeling arbitrary modality combination via the flexible mixture-of-experts,” in *NeurIPS*, 2024.

[46] X. Han, H. Nguyen, C. Harris, N. Ho, and S. Saria, “Fusemoe: Mixture-of-experts transformers for fleximodal fusion,” in *NeurIPS*, 2024.

[47] Z. Wang, C. Li, A. Zheng, R. He, and J. Tang, “Interact, embed, and enlarge: Boosting modality-specific representations for multi-modal person re-identification,” in *Proceedings of the AAAI Conference on Artificial Intelligence*, 2022, pp. 2633–2641.

[48] J. Crawford, H. Yin, L. McDermott, and D. Cummings, “Unicat: Crafting a stronger fusion baseline for multimodal re-identification,” *arXiv preprint arXiv:2310.18812*, 2023.

[49] Z. Wang, H. Huang, A. Zheng, and R. He, “Heterogeneous test-time training for multi-modal person re-identification,” in *Proceedings of the AAAI Conference on Artificial Intelligence*, 2024, pp. 5850–5858.

[50] Z. Yu, Z. Huang, M. Hou, Y. Yan, and Y. Liu, “Wtsf-reid: Depth-driven window-oriented token selection and fusion for multi-modality vehicle re-identification with knowledge consistency constraint,” *Expert Systems with Applications*, vol. 274, p. 126921, 2025.

[51] A. Liu, B. Feng, B. Xue, B. Wang, B. Wu, C. Lu, C. Zhao, C. Deng, C. Zhang, C. Ruan, *et al.*, “Deepseek-v3 technical report,” *arXiv preprint arXiv:2412.19437*, 2024.

[52] Z. Zhong, L. Zheng, G. Kang, S. Li, and Y. Yang, “Random erasing data augmentation,” in *Proceedings of the AAAI Conference on Artificial Intelligence*, 2020, pp. 13 001–13 008.

[53] L. Van der Maaten and G. Hinton, “Visualizing data using t-sne,” *Journal of machine learning research*, vol. 9, no. 11, 2008.

A Datasets Scale and Implementation Details

A.1 Datasets Scale

Table 6: Statistical analysis of datasets used in our experiments.

| Datasets | Object Type | # Samples | # IDs | # Cams |
|----------------|-------------|-----------|-------|--------|
| RGBNT201 [14] | Person | 4,787 | 201 | 4 |
| MSVR310 [13] | Vehicle | 2,087 | 310 | 8 |
| RGBNT100 [12] | Vehicle | 17,250 | 100 | 8 |
| WMVEID863 [15] | Vehicle | 4,709 | 863 | 8 |

We list the dataset statistics in Table 6, including the number of samples, identities, and cameras across these datasets. RGBNT201 [14] focuses on person ReID with four non-overlapping camera views and samples composed of RGB, NIR, and TIR modalities. MSVR310 [13] captures vehicles from eight unique angles over extended durations. RGBNT100 [12] provides diverse vehicle pairs across three spectra. WMVEID863 [15] serves as the largest available tri-spectral vehicle dataset with harsh lighting challenges.

A.2 Implementation Details

We resize each spectral image to 256×128 for person samples, and 128×256 for vehicle samples. Data augmentation includes random horizontal flipping, padding, cropping, and erasing [52]. We utilize the vision and text encoders in CLIP as the backbone, freezing all parameters of the text branch for text semantic projection, while keeping the visual branch fully trainable. Adam optimizer is used with the learning rate of $3.5e-6$, weight decay of 0.0001, and momentum set to 0.9. All experiments are conducted on one NVIDIA RTX 4090 GPU using the PyTorch framework.

B Ablation Studies

Table 7: Ablation studies of different modules on MSVR310 and RGBNT201.

| | Modules | | | MSVR310 | | | | RGBNT201 | | | |
|---|---------|------|------|-------------|-------------|-------------|-------------|-------------|-------------|-------------|-------------|
| | MMFA | TMSE | CSSE | mAP | R-1 | R-5 | R-10 | mAP | R-1 | R-5 | R-10 |
| A | ✗ | ✗ | ✗ | 50.1 | 68.9 | 83.4 | 87.8 | 71.0 | 73.6 | 84.2 | 88.2 |
| B | ✓ | ✗ | ✗ | 55.0 | 73.3 | 86.8 | 91.7 | 74.2 | 76.6 | 87.8 | 91.3 |
| C | ✓ | ✓ | ✗ | 59.7 | 75.1 | 88.2 | 92.0 | 78.9 | 84.4 | 91.1 | 93.2 |
| D | ✓ | ✓ | ✓ | 60.8 | 79.0 | 89.2 | 92.2 | 82.4 | 86.6 | 92.0 | 94.7 |

B.1 Effectiveness of Key Modules.

As shown in Table 7, to thoroughly validate the effectiveness of each proposed module, we conduct ablation studies on the vehicle dataset MSVR310 [13]. We also provide the complete ablation results on the RGBNT201 [14] dataset. In Row A, we use a three-branch CLIP visual encoder as the baseline, achieving 50.1% mAP and 68.9% Rank-1 accuracy on the vehicle dataset. By introducing the MMFA module, which treats each backbone feature as an independent expert, the performance improves to 55.0% mAP and 73.3% Rank-1. Further adding TMSE semantic experts brings an additional **+4.7%** mAP and **+1.8%** Rank-1 improvement. Finally, the CSSE structural experts boost performance to an optimal of **60.8%** mAP and **79.0%** Rank-1. These results validate the effectiveness and generalizability of each proposed component.

B.2 Effectiveness of Sampling Strategies

As shown in Table 8, we analyze different semantic expert sampling strategies on the RGBNT201 [14] dataset to evaluate their impact on model performance. In Row A, the All-Token strategy encodes all

Table 8: Effectiveness of sampling strategies.

| | Methods | mAP | R-1 |
|---|-------------------|-------------|-------------|
| A | All-Token | 79.0 | 83.0 |
| B | Top- K | 81.4 | 84.3 |
| C | Fixed- σ | 80.3 | 85.0 |
| D | σ_m (Ours) | 82.4 | 86.6 |

Table 9: Effectiveness of caption quality.

| Methods | Caption | mAP | R-1 |
|---------|-----------|-------------|-------------|
| IDEA | IDEA-Text | 80.2 | 82.1 |
| | NEXT-Text | 80.2 | 84.0 |
| NEXT | IDEA-Text | 80.5 | 84.7 |
| | NEXT-Text | 82.4 | 86.6 |

patch tokens $\mathbf{F}_{I,m}^{\text{tok}}$ for multi-modal fusion, but fails to identify key semantic regions across modalities, resulting in significant performance degradation. Row B adopts the Top- K strategy, replacing the dynamic routing threshold σ_m in \mathbf{R}_m with the top 50% tokens, achieving a suboptimal result of 81.4% mAP and 84.3% Rank-1. Row C replaces the dynamically generated threshold from $\mathbf{f}_{I,m}^{\text{cls}}$ with a fixed value (Fixed- σ), which lacks adaptive perception and relies on handcrafted heuristics, leading to inferior performance. In contrast, our proposed dynamic sampling strategy enables optimal performance, demonstrating its effectiveness in semantic sampling routing.

B.3 Effectiveness of Caption Quality

Table 9 presents an analysis on the RGBNT201 [14] dataset, evaluating the impact of caption quality on model performance. Compared with the captions used in IDEA, our high-quality captions lead to improved Rank-1 accuracy for the IDEA framework. Conversely, applying IDEA’s captions in our NEXT model results in a -1.9% drop in both mAP and Rank-1. These results demonstrate that caption quality plays a critical role in caption-based methods and highlight the effectiveness of our caption generation approach in NEXT.

C Reliable Caption Generation

Thanks to the powerful semantic generalization capability of Multi-modal Large Language models (MLLMs), we can leverage their out-of-the-box ability to generate comprehensive textual semantic descriptions about the object appearance. However, simple template-based text generation methods [23] face many practical challenges when deal with multi-modal data, such as noise interference from low-quality images and significant style discrepancies in some modalities, making it difficult to obtain clear object textual descriptions. To this end, our proposed approach firstly employs multiple MLLMs to generate a collection of attributes with confidence scores, and secondly we leverage the confidence scores with a multi-modal attributes aggregation strategy to generate clear and comprehensive object identity textual descriptions.

Confidence-aware Attributes Generation. To flexibly analyze the appearance information of the object, we use the generation of identity attributes as the basic step of reliable caption generation. We first define an instruction template to guide multiple MLLMs (e.g., GPT-4o [34], Qwen-VL [35], etc.) in structuring the attribute set of the input image. However, simple structured attribute information cannot quantitatively measure the confidence level of each item, the model suffers from low-quality visual modality noise, which leads to incorrect attribute selection. To address this, we introduce the concept of *confidence* score in the instruction template (See Template 6 and 7 for the full attribute template.) This allows us to observe the confidence level of each MLLM assigns to its output for each attribute. Additionally, to avoid the model ignoring environment information, we not only structure the output of ‘age’, ‘gender’, ‘upper clothing’, ‘lower clothing’, ‘hairstyle’, ‘footwear’ and other appearance attributes (in the case of pedestrian), but also require the MLLMs to output ‘view’, ‘illumination’, ‘capture time’, and ‘target clarity’ attributes to aware environmental information.

Multi-Modal Attributes Aggregation. Based on the structured attribute set with confidence score, we are able to further generate reliable captions for the object. However, as shown in Fig. 2, the RGB modal is affected by lighting degradation, causing the MLLMs to fail recognize the ‘backpack’ attribute. In contrast, the thermal infrared modality for the same identity easily reveals additional ‘backpack’ attribute. This leads to the model generating vague and incomplete textual captions such as ‘unknown’, ‘unclear’, or ‘not carrying’ based on mono visual modality. To address this problem,

Attribute Template (Pedestrian)

You are a visual analysis assistant specialized in processing images. Analyze the provided image and identify the most obvious person using the following attribute template. If the image is in visible light, include clothing color details. Output your result strictly as valid JSON. For each attribute, include a "value" (selected from the provided options or descriptive text), a "confidence" score between 0 and 1.

```
{  
  "age": {"value": "child | teenager | adult | senior", "confidence": 0.0},  
  "gender": {"value": "male | female | non-binary", "confidence": 0.0},  
  "view": {"value": "front | back | side", "confidence": 0.0},  
  "illumination": {"value": "bright | normal | dim", "confidence": 0.0},  
  "capture_time": {"value": "daytime | nighttime | unclear", "confidence": 0.0},  
  "target_clarity": {"value": "clear | blurry", "confidence": 0.0},  
  "upper_clothing": {"value": "e.g., t-shirt | sweater | jacket", "confidence": 0.0},  
  "upper_clothing_color": {"value": "e.g., red, blue, green", "confidence": 0.0},  
  "lower_clothing": {"value": "e.g., jeans | shorts | skirt", "confidence": 0.0},  
  "lower_clothing_color": {"value": "e.g., black, blue", "confidence": 0.0},  
  "hair_length": {"value": "short | medium | long", "confidence": 0.0},  
  "hair_style": {"value": "e.g., straight | curly", "confidence": 0.0},  
  "footwear": {"value": "e.g., sneakers | sandals", "confidence": 0.0},  
  "footwear_style": {"value": "e.g., casual | formal", "confidence": 0.0},  
  "carrying": {"value": "e.g., backpack | luggage | none", "confidence": 0.0},  
  "holding": {"value": "e.g., a phone | bottle | none", "confidence": 0.0},  
  "handbag": {"value": "carrying handbag | not", "confidence": 0.0},  
  "backpack": {"value": "carrying backpack | not", "confidence": 0.0},  
  "glasses": {"value": "wearing glasses | not", "confidence": 0.0},  
  "suitcase": {"value": "dragging | not dragging", "confidence": 0.0}  
}
```

Please provide the analysis in valid JSON only.

Figure 6: Instruction template for generating pedestrian attributes with confidence.

we propose a multi-modal attribute aggregation strategy based on confidence scores to preprocess semantic complementary information in different visual modalities.

(1) Multi-Modal Merge and Complement. Specifically, we first use multiple MLLMs to identify object attributes, and for each identified attribute we select the MLLMs with the highest confidence as their final value to improve the accuracy of each attribute within the modality. Furthermore, taking the RGB modality as an example, its modality-specific low-frequency attributes, such as '*illumination*,' '*upper clothing color*,' and '*lower clothing color*,' are easy to recognize. In contrast, attributes requiring high-frequency information, such as '*carrying*,' '*holding*,' '*handbag*,' and '*backpack*,' are often incorrectly recognized as '*unknown*,' '*unclear*,' or '*not carrying*.' This significantly affects the clarity of the final generated captions. To address this, we rely on the confidence scores to select the highest-confidence attributes from the NIR and TIR modalities, which are unaffected by lighting conditions, in order to recheck and complement the absent information. Similarly, we apply the same complementary strategy to each modality in order to obtain a complete and reliable set of attributes for each modality.

(2) Caption Generation. Building on the above complete attribute set, we define the following instruction template to guide the LLM [51] in combining the structured attribute set from each modality to generate the final text caption (See Template 8 and 9 for the full caption template.) Finally, we have constructed a complete and reliable caption generation pipeline, and we leverage the same process on vehicle datasets to obtain a comprehensive semantic description of the vehicle.

D Visualization Analysis

D.1 Feature Distribution

As shown in Fig. 10, to further investigate the impact of the proposed modules on model features, we visualize the feature distributions on the RGBNT201 [14] dataset using T-SNE. Comparing Fig. 10 (a) and 10 (b), the introduction of MMFA effectively aggregates different instances of the

Attribute Template (Vehicle)

You are a visual analysis assistant specialized in processing images. Analyze the provided image and identify the most obvious vehicle using the following attribute template. If the image is in visible light, include clothing color details. Output your result strictly as valid JSON. For each attribute, include a "value" (selected from the provided options or descriptive text), a "confidence" score between 0 and 1.

```
{  
  "vehicle_type": {"value": "e.g., sedan | SUV | truck | coupe | convertible | minivan | hatchback | motorcycle, etc", "confidence": 0.0},  
  "branding": {"value": "e.g., Volkswagen | Skoda | Mitsubishi | Mazda | Honda | Geely | Ford | Buick | BMW | Benz | Audi, etc", "confidence": 0.0},  
  "color": {"value": "red | blue | black | white | silver | gray | yellow | green | orange | brown | purple", "confidence": 0.0},  
  "view": {"value": "front | back | side | top | diagonal", "confidence": 0.0},  
  "illumination": {"value": "bright | normal | dim", "confidence": 0.0},  
  "capture_time": {"value": "daytime | nighttime | unclear", "confidence": 0.0},  
  "target_clarity": {"value": "clear | blurry", "confidence": 0.0},  
  "window_condition": {"value": "clear | tinted | broken | dirty | unclear", "confidence": 0.0},  
  "window_style": {"value": "flat | curved | panoramic", "confidence": 0.0},  
  "exterior_condition": {"value": "new | used | worn | damaged", "confidence": 0.0},  
  "headlights_shape": {"value": "round | oval | rectangular | angular", "confidence": 0.0},  
  "taillights_shape": {"value": "round | oval | rectangular | angular", "confidence": 0.0},  
  "front_grille_shape": {"value": "horizontal | vertical | hexagonal | angular", "confidence": 0.0},  
  "front_grille_edges": {"value": "sharp | rounded | straight | irregular", "confidence": 0.0},  
  "roof_type": {"value": "flat | sloped | sunroof | convertible | dome", "confidence": 0.0},  
  "roof_condition": {"value": "clean | dirty | damaged", "confidence": 0.0},  
  "tires_type": {"value": "all-terrain | street | off-road | winter | regular", "confidence": 0.0},  
  "tires_condition": {"value": "new | worn | damaged", "confidence": 0.0},  
  "tire_size": {"value": "small | medium | large", "confidence": 0.0},  
  "headlights_condition": {"value": "on | off | dimmed | broken", "confidence": 0.0},  
  "bumper_condition": {"value": "intact | damaged | missing", "confidence": 0.0},  
  "license_plate": {"value": "visible | not visible", "confidence": 0.0},  
  "spoiler": {"value": "present | not present", "confidence": 0.0},  
  "roof_rack": {"value": "present | not present", "confidence": 0.0},  
  "side_mirrors": {"value": "present | not present", "confidence": 0.0},  
  "side_mirror_condition": {"value": "intact | broken | missing", "confidence": 0.0},  
  "exhaust_type": {"value": "single | dual | hidden", "confidence": 0.0}  
}
```

Please provide the analysis in valid JSON only.

Figure 7: Instruction template for generating vehicle attributes with confidence.

Caption Template (Pedestrian)

Generate a natural person appearance description by strictly following this template and using ONLY the highest-confidence attributes from the provided JSON data (ignore any with 0 confidence).

'A [age] [gender] seen from the [view] during [capture_time] in [illumination] lighting. [gender:male|He][gender:female|She][gender:non-binary|The person] is wearing a [upper_clothing_color] [upper_clothing] with [lower_clothing_color] [lower_clothing], paired with [footwear_style] [footwear]. [Hair_length] [hair_style] hair [glasses: wearing glasses|glasses: not wearing glasses] and [gender:male|He][gender:female|She][gender:non-binary|the person] is wearing glasses]. [gender:male|He][gender:female|She][gender:non-binary|The person] is [carrying a [carrying] | holding a [holding] | [handbag] | [backpack] | [suitcase]]. The image appears [target_clarity].'

Do not include any introductory text, titles, explanations, or content outside this template structure.

Figure 8: Instruction template for generating pedestrian caption.

Caption Template (Vehicle):

Generate a natural vehicle appearance description by strictly following this template. Always use highest-confidence values from these two JSON datasets of the same vehicle (ignore confidence=0). ‘A [color] [branding] [vehicle_type] viewed from the [view] in [illumination] [capture_time] light (image appears [target_clarity]). The vehicle shows [exterior_condition] wear with [window_condition] [window_style] windows. It features [headlights_condition] [headlights_shape] headlights and [taillights_shape] taillights, complemented by a [front_grille_shape] grille with [front_grille_edges] edges. The [roof_condition] [roof_type] roof sits above [tires_condition] [tire_size] [tires_type] tires with [bumper_condition] bumpers. [Side mirrors are [side_mirror_condition].] [License plate is [license_plate].] [Spoiler is [spoiler].] [Roof rack is [roof_rack].] [Exhaust system features [exhaust_type] pipes.]’ Omit any bracketed sections where data is unavailable. Do not include any introductory text, titles, explanations, or content outside this template structure.

Figure 9: Instruction template for generating vehicle caption.

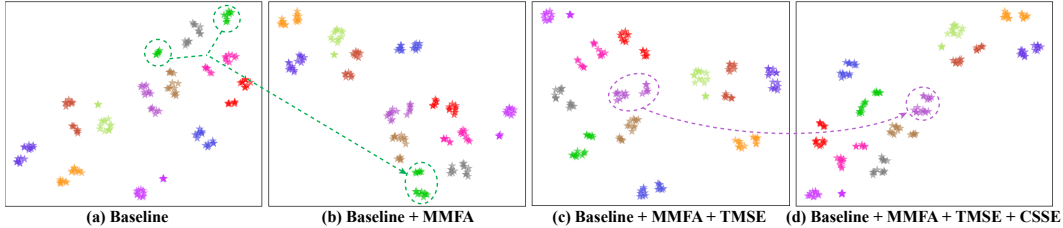


Figure 10: T-SNE [53] visualization of the feature distribution on RGBNT201 [14] (a) Baseline, (b) Baseline + MMFA, (c) Baseline + MMFA + TMSE, and (d) Baseline + MMFA + TMSE + CSSE (Ours).

same identity. As illustrated in Fig. 10 (c), incorporating the TMSE semantic experts improves the separability of samples across identities. In Fig. 10 (d), the inclusion of CSSE structural experts leads to tighter clustering of difficult identity samples, resulting in well-separated intra-class and inter-class distributions. These results validate the effectiveness of each proposed module.

D.2 Expert Feature Visualization

As shown in Fig. 11 and Fig. 12, to further explore the recognition and perception capabilities of each expert, we visualize the sampled tokens of semantic experts and the activated regions of structural experts. Clearly, we observe that each semantic expert $\mathbf{E}_T = \{E_t^{(1)}, E_t^{(2)}, \dots, E_t^{(N_T)}\}$ tends to focus on tokens related to the object, which allows the experts to attend to distinct semantic parts. Moreover, each semantic expert preferentially samples tokens from different spectral modalities. The semantic experts effectively sample complementary tokens across modalities, demonstrating their ability to perceive fine-grained object parts and extract multi-modal features under text modulation. Furthermore, as illustrated in Fig. 11 and Fig. 12, we observe that structural experts $\mathbf{E}_C = \{E_c^{(1)}, E_c^{(2)}, \dots, E_c^{(N_C)}\}$ consistently perceive the complete structure within modalities, maintaining coarse-grained structural features of the object. These visualizations strongly support the effectiveness of NEXT’s multi-grained expert design that models ReID through semantic sampling and structural perception.

D.3 Retrieval Results

To verify the model’s effectiveness in real-world scenarios, we visualize the retrieval results of models with different module combinations on the RGBNT201 [14] and MSVR310 [13] datasets and compare NEXT with state-of-the-art methods [18, 23, 24]. As shown in Fig. 13, on the RGBNT201 [14] dataset, the introduction of different modules enables the model to more effectively recognize pedestrians with the same identity. Fig. 14 compares NEXT with existing state-of-the-art methods, demonstrating that NEXT achieves superior retrieval performance for target pedestrians under various low-light conditions. In Fig. 15, on the MSVR310 [13] dataset, the model’s ability to identify challenging vehicles progressively improves with the addition of different components. Fig. 16 compares NEXT



Figure 11: Visualization of the sampled patch tokens and activated feature regions for experts on RGBNT201 [14].

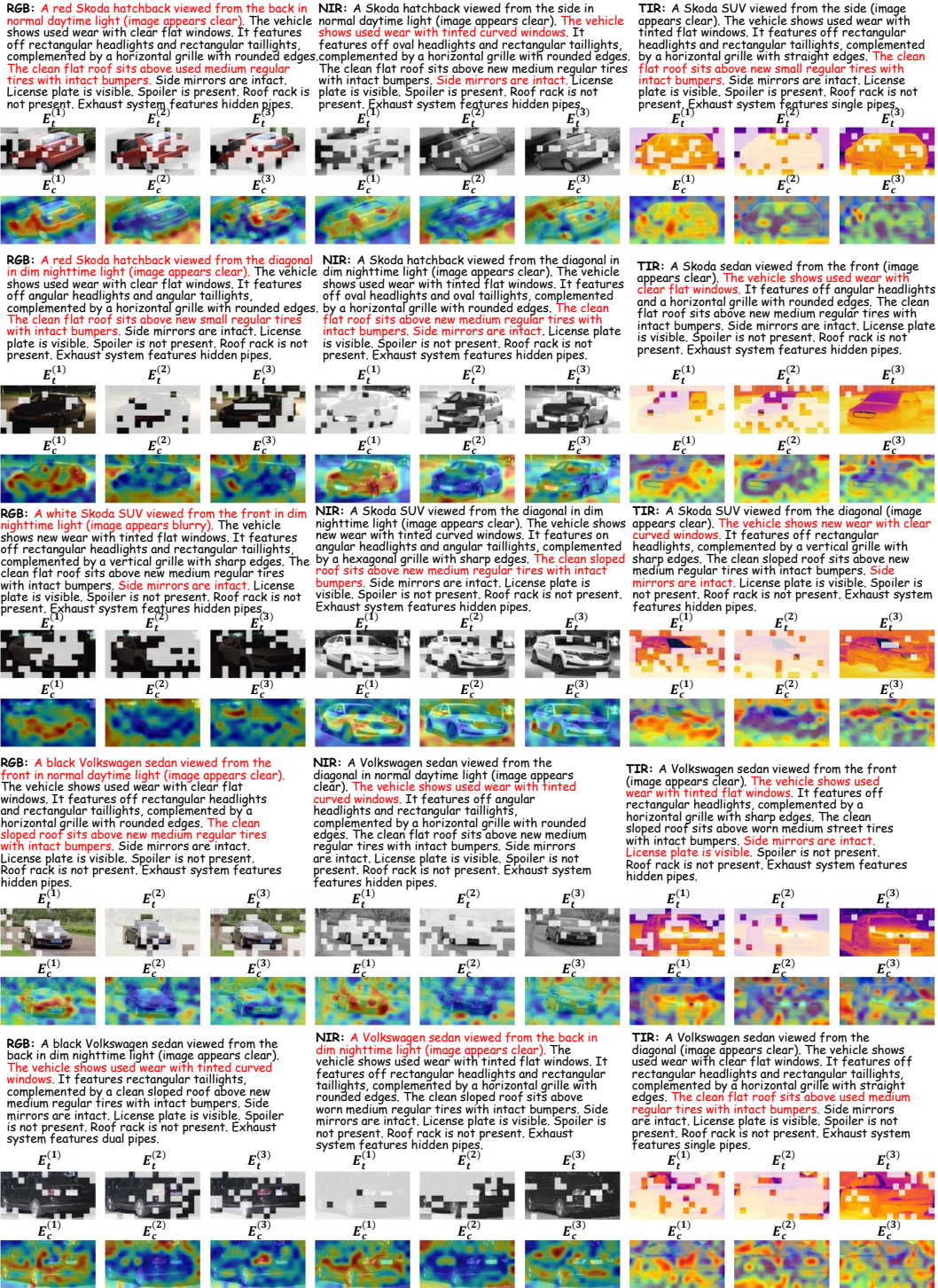


Figure 12: Visualization of the sampled patch tokens and activated feature regions for experts on MSVR310 [13].

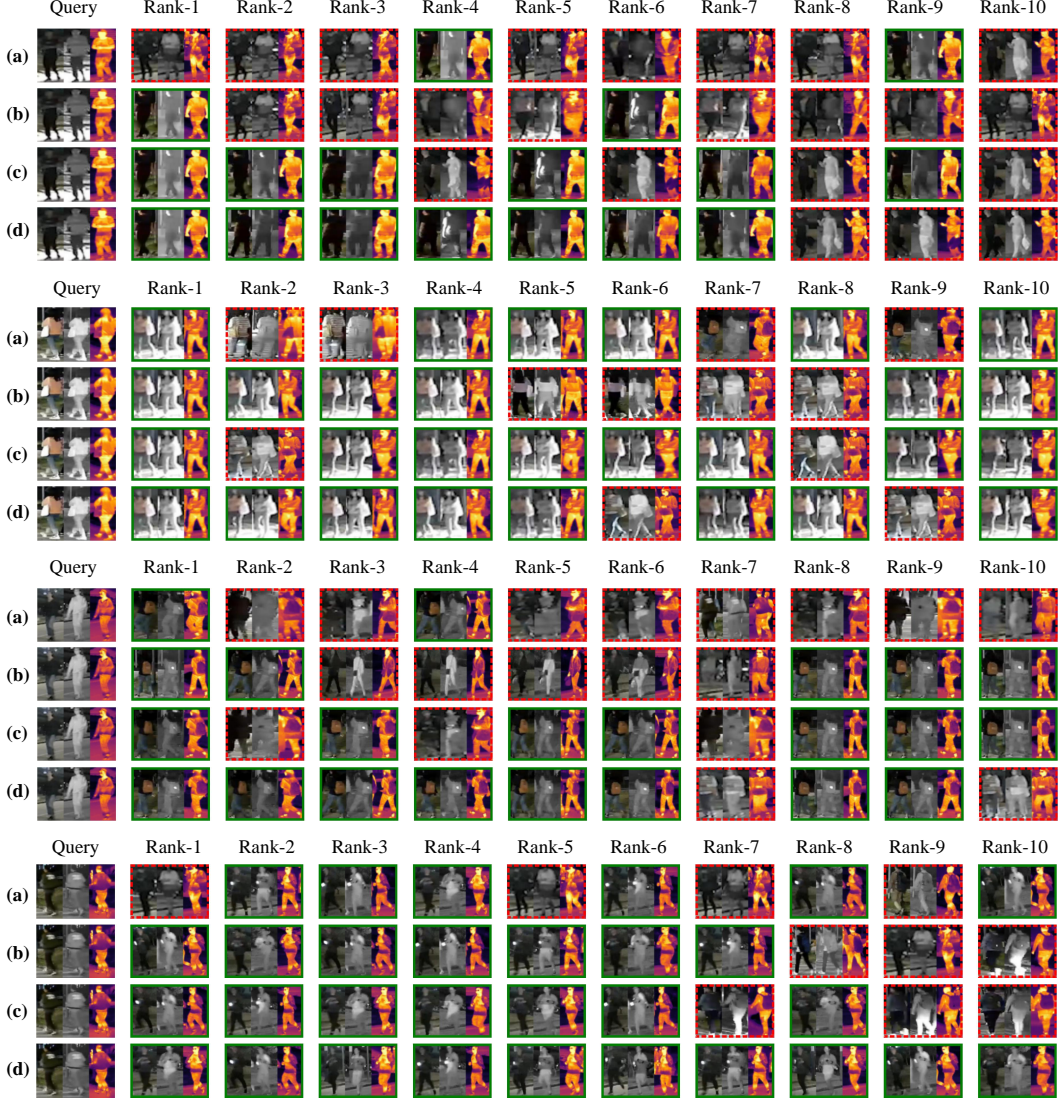


Figure 13: Visualization of the retrieval results on RGBNT201 [14] (a) Baseline, (b) Baseline + MMFA, (c) Baseline + MMFA + TMSE, and (d) Baseline + MMFA + TMSE + CSSE (Ours).

to current state-of-the-art methods, showing that NEXT effectively leverages multi-modal data to overcome challenges in low-light and cross-day-night scenarios, accurately identifying vehicles.

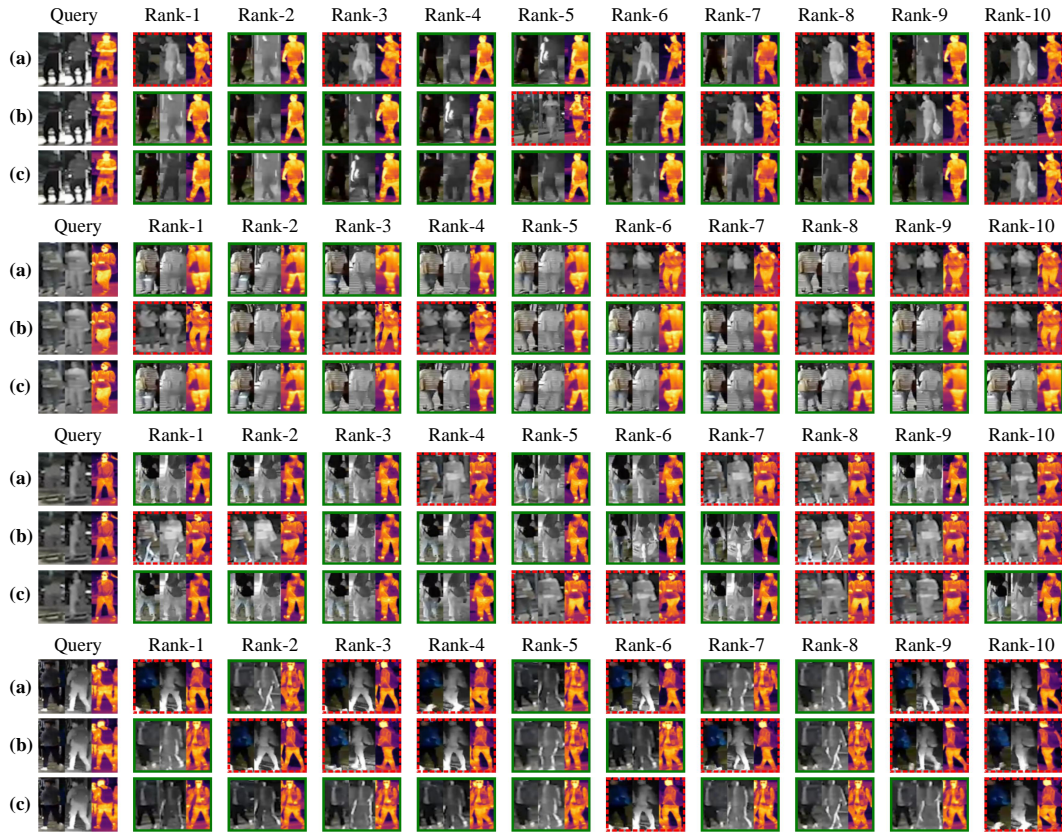


Figure 14: Visualization of the retrieval results on RGBNT201 [14] (a) DeMo [18], (b) IDEA [23], and (c) NEXT (Ours).

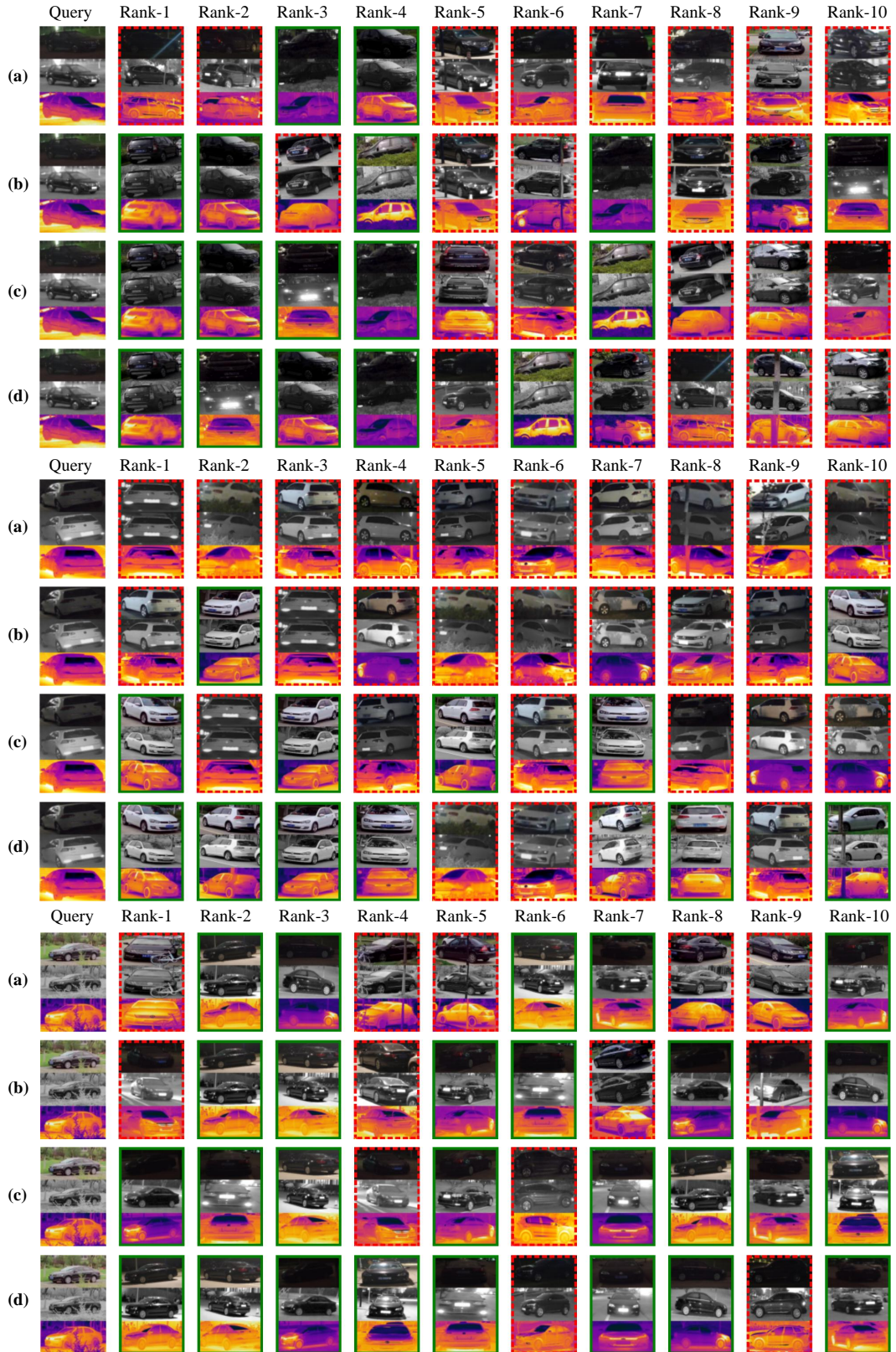


Figure 15: Visualization of the retrieval results on MSVR310 [13] (a) Baseline, (b) Baseline + MMFA, (c) Baseline + MMFA + TMSE, and (d) Baseline + MMFA + TMSE + CSSE (Ours).



Figure 16: Visualization of the retrieval results on MSVR310 [13] (a) DeMo [18], (b) ICPL-ReID [24], and (c) NEXT (Ours).